

Experimental Investigation of Gas/Slag/Matte/Spinel Equilibria in the Cu-Fe-O-S-Si System at 1473 K (1200 °C) and $P(\text{SO}_2) = 0.25$ atm



TAUFIQ HIDAYAT, ATA FALLAH-MEHRJARDI, PETER C. HAYES,
and EVGUENI JAK

New experimental data were obtained on the gas/slag/matte/spinel equilibria in the Cu-Fe-O-S-Si system at 1473 K (1200 °C) and $P(\text{SO}_2) = 0.25$ atm covering Cu concentrations in matte between 42 and 78 wt pct Cu. Accurate measurements were obtained using high-temperature equilibration and the rapid quenching technique, followed by electron-probe X-ray microanalysis of equilibrium phase compositions. The use of spinel substrates made to support the samples ensures equilibrium with this primary phase solid, eliminates crucible contamination, and facilitates direct gas–condensed phase equilibrium and high quenching rates. Particular attention was given to the confirmation of the achievement of equilibrium. The results quantify the relationship between Cu in matte and oxygen partial pressure, sulfur in matte, oxygen in matte, Fe/SiO₂ at slag liquidus, sulfur in slag, and dissolved copper in slag.

<https://doi.org/10.1007/s11663-018-1262-3>

© The Minerals, Metals & Materials Society and ASM International 2018

I. INTRODUCTION

FUNDAMENTAL accurate information on the gas/slag/matte equilibria in the Cu-Fe-O-S-Si system is essential for understanding and improving the existing and for developing new high-temperature copper production processes. Most of the previous investigations of slag/matte equilibria at controlled sulfur dioxide partial pressures $P(\text{SO}_2)$ have been carried out at tridymite saturation.^[1–10] Those studies used either large crucibles with the bulk chemical analysis method^[1–8] or substrates with the microanalysis technique.^[9,10] Spinel is a common solid found in equilibrium with matte and slag phases in industrial furnaces.^[9,11] Only a few studies provide data on the equilibria between matte and spinel at fixed $P(\text{SO}_2)$.^[12–15] Not many attempts were made to investigate the equilibria in the slag/matte/spinel at controlled gas atmosphere.^[16,17] This is due to difficulty in performing experiments, since the system contains aggressive slag and matte liquids. The aim of the present

study is to accurately measure the gas/slag/matte/spinel equilibria in the Cu-Fe-O-S-Si system at 1473 K (1200 °C), $P(\text{SO}_2) = 0.25$ atm, and over a range of oxygen partial pressure $P(\text{O}_2)$. These data are essential to characterize the relationships between oxygen partial pressure, matte composition, and slag composition in the presence of spinel solid.

II. EXPERIMENTAL METHODOLOGY AND COMPOSITIONAL ANALYSIS OF PHASES

The experimental methodology used in this study is based on the general approach developed by the authors^[18,19] involving high-temperature equilibration using a spinel substrate in a vertical tube furnace under controlled gas atmospheres (20 pct CO–80 pct Ar/CO₂/SO₂), rapid quenching of the equilibrated phases, metallographic preparation of samples, and direct measurement of the compositions of the equilibrium phases with electron-probe X-ray microanalysis (EPMA). Detailed description of the development of the specific experimental methodology for the gas/slag/matte/tridymite equilibria in the Cu-Fe-O-S-Si system was given in previous publications by Fallah *et al.*^[20,21] The methodology used in the present study follows the approach described by Fallah *et al.*, the study on the gas/matte/spinel equilibria in the Cu-Fe-O-S system,^[22] and initial studies of gas/matte/slag/spinel equilibria in the Cu-Fe-O-S-Si system.^[23,24]

TAUFIQ HIDAYAT, PETER C. HAYES, and EVGUENI JAK are with the Pyrometallurgy Innovation Centre (PYROSEARCH), School of Chemical Engineering, The University of Queensland, Brisbane, QLD 4072, Australia. Contact e-mail: t.hidayat@uq.edu.au ATA FALLAH-MEHRJARDI is with Research Development and Innovation, Aurubis AG, Hamburg, Germany, and also with the Pyrometallurgy Innovation Centre (PYROSEARCH), School of Chemical Engineering, The University of Queensland.

Manuscript submitted August 22, 2017.

Article published online April 24, 2018.

Before undertaking the experimental studies, a degree of freedom analysis of the system was undertaken, assuming $F = C + 2 - P$, where C = number of component, P = number of phases, and F = number of degrees of freedom. For the Cu-Fe-O-S-Si-Ar-C system, $F = 7$ (Cu, Fe, Si, O, S, C, Ar) + 2 - 4 (gas, slag, matte, spinel) = 5. The fixed degrees of freedom are (1) constant temperature, (2) total pressure of 1 atm, (3) constant $P(\text{SO}_2)$, (4) constant $P(\text{Ar})$, and (5) fixed $P(\text{O}_2)$. Thus, the system was fully specified, so that all variables, *i.e.*, matte composition, slag composition, and partial pressures of other gas species ($P(\text{CO})$, $P(\text{CO}_2)$, and $P(\text{S}_2)$), were defined. The $P(\text{O}_2)$, $P(\text{SO}_2)$, and $P(\text{Ar})$ were set by the controlled proportion of 20 pct CO-80 pct Ar, CO_2 , and SO_2 gas flows. Variation of the last degree of freedom, $P(\text{O}_2)$, when all others are kept constant, provides an unambiguous way to represent all properties of the system as a function of one selected variable. In the present study, the variable of choice for an X -axis was Cu in matte (Cu in matte is defined as $100 \cdot \text{Cu} / [\text{Cu} + \text{Fe} + \text{S}]$ by weight).

In the present study, spinel (Fe_3O_4) substrates were used to support the slag and matte samples. The spinel was prepared from the 99.5 wt pct pure iron foil (supplied by Goodfellow Cambridge Ltd., Huntingdon, England) folded into the required shape and then oxidized. Two different oxidation conditions were used to prepare spinel: (1) at 1473 K (1200 °C) for 2 hours using $\text{CO}/\text{CO}_2/\text{Ar}$ gas corresponding to $P(\text{O}_2) = 10^{-8.5}$ atm (spin 1) and (2) at 1473 K (1200 °C) for 2 hours using pure CO_2 gas corresponding to $P(\text{O}_2) = 10^{-3.87}$ atm (spin 2). Based on previous assessment of the Fe-O system,^[25] both conditions are expected to produce close to stoichiometric Fe_3O_4 .

Several different shapes of spinel substrates were tested. The final substrate shape adopted was in the form of an envelope with open ends.^[23] The other type of spinel substrate used in the present study during confirmation experiments by an independent researcher was the spiral shape.^[23] The total mass of slag and matte is approximately 0.6 g, resulting in thin films of equilibrated condensed phases in contact with both the solid substrates and the gas phase. The technique gives advantages compared to the conventional approach of using bulk refractory crucibles, since the sample has direct exposure to gas, the rate of quenching of the sample is rapid, and contamination of the sample by unwanted elements is avoided.

For EPMA, a JEOL* JXA 8200L was used for phase

*JEOL is a trademark of Japan Electron Optics Ltd., Tokyo.

composition measurements at an acceleration voltage of 15 kV and a probe current of 15 nA. The Duncumb-Philibert ZAF correction procedure supplied with the JEOL JXA 8200L probe was applied. The reference materials from Charles M. Taylor (Stanford, CA) used as standards were chalcopyrite CuFeS_2 for Cu, Fe, and S in matte and S in slag, quartz SiO_2 for Si in slag and spinel, and hematite Fe_2O_3 for Fe in slag and spinel.

Cuprite Cu_2O standard purchased from Structure Probe Inc. (PA, USA) was used for Cu in slag and spinel. Fully focused or zero-diameter beam was used for the EPMA compositional measurement of the spinel phase. The slag phase was sometimes found to be heterogeneous, containing copper-rich precipitates. The matte phase was also found to be heterogeneous, containing high-copper veins within the matte matrix formed during cooling of the samples. Nonzero probe diameter with take-off area between 10 and 50 μm , therefore, was used to obtain the mean compositions of the slag and matte phases. The increase of the probe diameter from fully focused electron beam to 50 μm decreased the uncertainty of the phase composition and did not affect the accuracy; detailed analysis of the uncertainties and standard deviations associated with these measurements was given in a previous study.^[20] Only concentrations of metal cations and sulfur in the phases were measured by the EPMA in the present study; all concentrations in liquid slag and solid oxides were recalculated to selected oxidation states (*i.e.*, Cu_2O , FeO , SiO_2 , and S) and normalized for presentation purposes, to unambiguously report the compositions of the phases and for consistency with previous publications.^[20-24] The normalized compositions and original sums of elements or oxides from EPMA analyses are provided in tabular form.

III. CONFIRMATION OF THE ACHIEVEMENT OF EQUILIBRIUM

The achievement of equilibrium was tested based on the four-point-test approach, involving the following: (1) evaluation of the influence of equilibration time, (2) assessment of phase homogeneity, (3) approaching equilibrium from different directions, and (4) systematic analysis of reactions specific to the system. The study also included equilibrium tests with different starting materials, analysis of solid-state diffusion of solutes in spinel solid, and confirmation experiments by an independent researcher.

A. Description of Key Reactions and Elementary Processes Taking Place during the Equilibration Process

A number of elementary reactions and mass transfer processes take place simultaneously during the equilibration process. Analysis of their effects on the equilibration process is important to avoid any barrier in the equilibration process, to improve the experimental design, and to ensure that the appropriate strategy is used to achieve the final equilibrium point within the required time. Figure 1 illustrates possible mass transfer pathways of various species in the gas, slag, matte, and spinel phases, resulting from the reactions at each interface and following the overall Cu, Fe, S, O, and Si elemental mass balances. Several possible elementary reactions taking place during the gas/slag/matte/spinel equilibration in the Cu-Fe-O-S-Si system were proposed. Based on general knowledge of the investigated system and previous publications,^[20,22] some selected reactions/processes are listed subsequently:

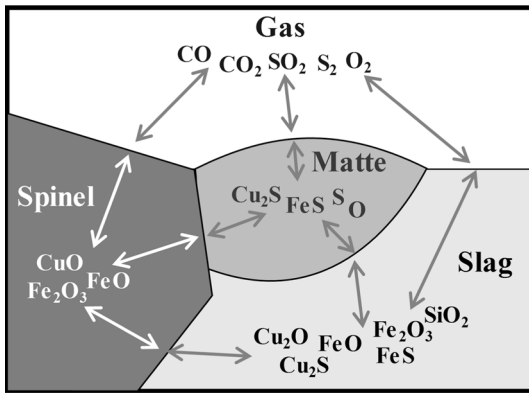
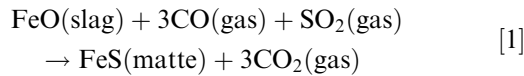
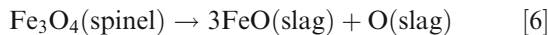
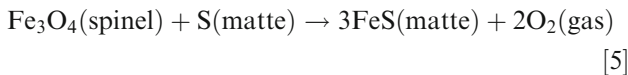
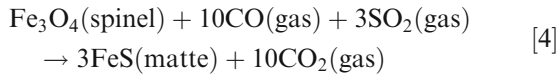


Fig. 1—Schematic of mass transfer pathways of the predominant species in gas, slag, matte, and spinel phases involved in reactions between these phases.



Mass transfer of Cu, Fe, and O within the matte phase [2]

Mass transfer of Cu, Fe, S, O, and Si within the slag phase [3]



Note that this list of reactions is not meant to be complete and is introduced only to facilitate analysis of the overall combination of processes taking place during equilibration.

Since only the Fe concentration is relatively high in all condensed phases (slag, matte, and spinel), the overall combination of reactions and mass transfer between the gas, matte, and slag phases taking place during equilibration may be approximately described through the simplified iron exchange Reaction [1] or reverse of Reaction [1]. This reaction involving three different phases represents a combination of (1) the reactions taking place in the three-phase contact areas, (2) reactions taking place at the two-phase interfaces, (3) reactions in the single phase, and (4) the corresponding mass transfer of Cu, Fe, and O within the matte phase (Reaction [2]) and of Cu, Fe, S, O, and Si

within the slag phase (Reaction [3]). The reaction/mass transfer between the gas, matte, and spinel phases can also take place through the iron exchange (Reaction [4] or [5] or reverse of Reaction [4] or [5]) at the interface of the matte and spinel phases. All changes occurring in the sample due to Reactions [1, 4, 5] lead to either spinel dissolution or crystallization according to Reaction [6].

B. Reaction Pathways Toward Final Equilibrium Point

The previous experimental study of gas/matte/spinel equilibria in the Cu-Fe-O-S system^[22] demonstrated that final equilibrium could be readily approached from starting conditions of higher or lower Cu in matte (Cu in matte is defined as $100 \cdot \text{Cu}/[\text{Cu} + \text{Fe} + \text{S}]$ by weight). In samples moving from low to high Cu in matte, the precipitation of Fe_3O_4 was observed as a result of the equilibration process. In samples moving from high to low Cu in matte, the spinel solids formed irregular shape of the interface of the substrate, indicating the dissolution process of Fe_3O_4 into the Cu_2S -FeS matte.

As described previously,^[22] it was decided to approach the equilibrium point using starting mixtures having Cu in matte close to and lower than that of the final matte composition. Although a spinel rim was formed on the surface of matte, free surface of matte exposed to the gas phase was still observed. The precipitation of solid is preferred since it ensures the formation of the equilibrium spinel. This approach also gives a high success rate of experiments by avoiding the dissolution and failure of the spinel substrate.

C. Trend of Compositions at Different Locations and Equilibration Times

A series of experiments at 1473 K (1200 °C), $P(\text{SO}_2) = 0.25$ atm, and $P(\text{O}_2) = 10^{-8.5}$ atm with different equilibration times (0.5, 3, 24, and 48 hours) was performed with the initial mixture shown in Table I. Spinel substrates from the oxidation of iron foils at 1473 K (1200 °C) and $P(\text{O}_2) = 10^{-8.5}$ atm were used (spin 1) in this preliminary experiment.

The mass balance model described in a previous publication^[20] was used to predict the initial phase compositions and proportions of slag, matte, and possible interactions between the crucible and the slag phase. The model was based on the assumptions that (1) the reactions between the condensed phases (especially between slag and matte phases) took place rapidly and were completed in the initial stages of the experiment and (2) the reactions between the gas phase and the condensed phases required longer times to complete. FactSage software** with public database^[26–30] was also

**FactSage software is developed by CRCT, Montreal, Canada and GTT-Technologies, Herzogenrath, Germany.

used to predict the starting phase compositions. The predicted interactions between the mixture and crucible

Table I. Initial Mixture Used in the Gas/Slag/Matte/Spinel Equilibria Experiment

Mixture	SiO ₂	Fe ₂ O ₃	FeO	FeS	Cu ₂ S	CuS	Total Weight (g)
Sulfides + oxides	0.71	0.35	1.64	0.26	0.45	0.56	3.96

Table II. Predicted Initial Cu in Matte and Crucible Interaction Based on the Mass Balance Calculation and FactSage Prediction^[26-30]

Mixture	Prediction Tool	Predicted Cu in Matte (Wt Pct)	Slag Proportion (Pct)	Slag/Crucible Interaction	SO ₂ Addition (g)	Fe/SiO ₂ in Slag (Wt/Wt)
Sulfides + oxides	mass balance	57.7	67.4	dissolving	- 0.1	2.14
	FactSage + public database ^[26-30]	58.2	68.1	dissolving	- 0.1	2.09

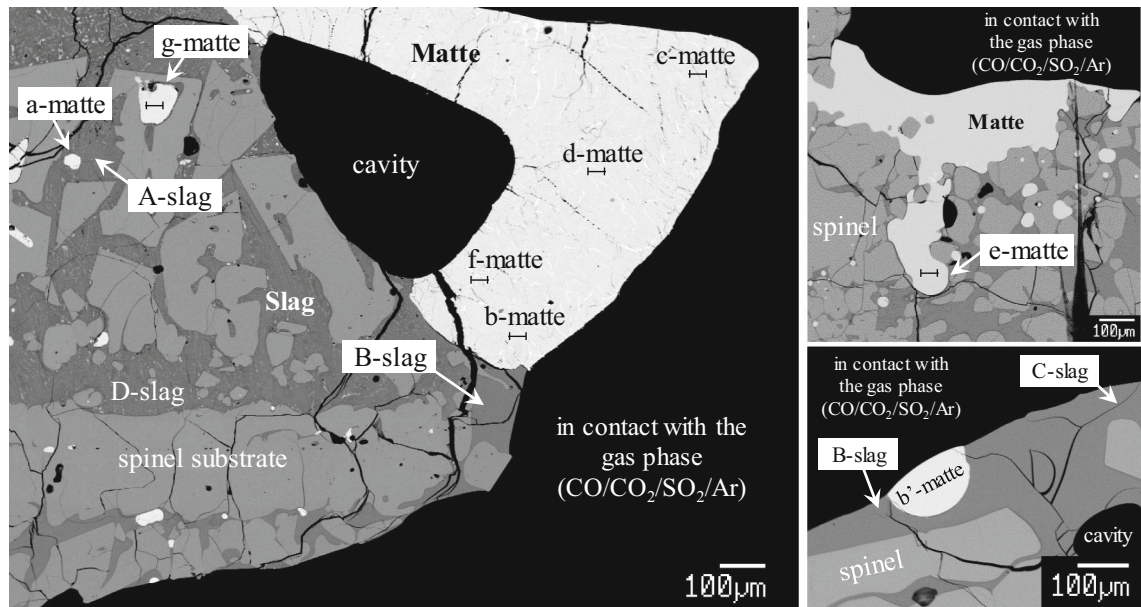


Fig. 2—SEM backscattered image showing examples of different locations and associations of matte, slag, and gas phases produced from gas/slag/matte/spinel equilibria in the Cu-Fe-O-S-Si system at 1473 K (1200 °C), $P(\text{SO}_2) = 0.25$ atm, and equilibration time between 0.5 and 24 h.

shown in Table I are provided in Table II. It can be seen that there are differences in the predicted matte and slag compositions between the mass-balance model and the FactSage prediction. The mass-balance model differs from the FactSage prediction since the model is based on the preliminary experimental results obtained in the present study. The initial mixture had excess of sulfur, as indicated by the predictions showing rejection of 0.1 g of SO₂.

The predictions of initial matte and slag compositions enable the starting point of the sample to be determined. The starting compositions are used for analysis of the compositional gradients in the sample. This analysis is performed in order to identify key reactions taking place during the equilibrium process, to understand inhomogeneity at micro- and macroscale that appear in the sample, to confirm the achievement of the final equilibrium, to ensure representative phases are measured, and finally to develop the appropriate experimental methodology specific to this system.

Figure 2 shows an example of an SEM backscattered image of an equilibrated sample in the gas/slag/matte/spinel equilibria. The label shows different locations and associations of slag, matte, and gas phases based on the classification given in Table III.^[20,22] The trends of compositions as functions of the phase locations (Table III) and various equilibration times were investigated and are summarized in Figure 3.

In the 0.5-hour experiment, the measured concentrations of Cu in matte were between 46 and 52 wt pct, significantly lower than the initially predicted composition of approximately 58 wt pct (Table II). The significant decrease of the Cu in matte below the expected initial composition was also observed in the previous study on the gas/matte/spinel equilibria.^[22] It was previously found that the movement toward the lower Cu in matte was related to the presence of wüstite phase in the spinel substrate from incomplete oxidation of Fe foil to spinel. The wüstite phase reacted with the CO/CO₂/SO₂ gas, forming Fe-S-O matte in the initial stage

Table III. Definition of the Various Types of Matte and Slag Phase Locations^[20,22]

Matte Terminology	Label	Slag Terminology	Label
Entrapped matte, droplet	a	slag-matte far from gas	A
Matte-gas exposure close to slag, chunky shape	b	slag-matte close to gas	B
Matte-gas exposure close to slag, small particles	b'	slag far from matte close to gas	C
Matte-gas exposure far from slag	c	slag far from matte far from gas	D
matte far from gas far from slag	d		
Matte far from gas close to slag, channel shaped	e		
Matte far from gas close to slag, chunky shaped	f		
Matte entrapped in spinel	g		

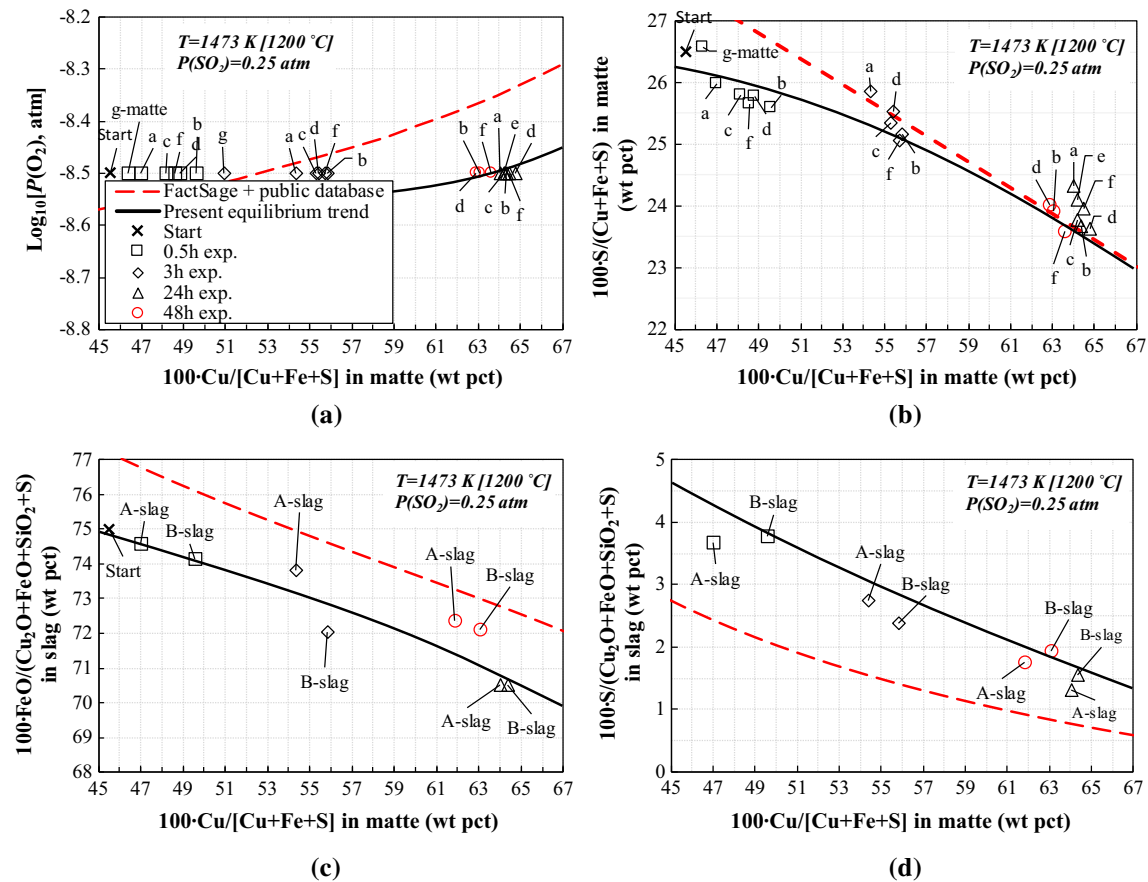


Fig. 3—Compositions of the matte and slag phases from different locations and equilibration times at 1473 K (1200 °C), $P(\text{SO}_2) = 0.25$ atm, and $P(\text{O}_2) = 10^{-8.5}$ atm: (a) oxygen partial pressure ($P(\text{O}_2)$, atm) vs Cu in matte; (b) concentration of sulfur in matte vs Cu in matte; (c) FeO in slag vs Cu in matte; and (d) concentration of sulfur in slag vs Cu in matte. Labels are locations of the phases described in Fig. 2. The “start” label in the graphs indicates the value of predicted starting composition. Dashed lines are FactSage predictions using the public database.^[26–30] Solid lines are present equilibrium trend lines obtained from experiments with equilibration times longer than 24 h.

of reaction. As time progressed, the FeS from the matte was fully converted to spinel. To avoid the formation of Fe-rich mattes from the spinel substrate, in further experiments, spinel substrates spin 2 prepared by oxidation of Fe foils at 1473 K (1200 °C) with pure CO_2 gas were used. At this condition, complete conversion of Fe to Fe_3O_4 was obtained within 2 hours oxidation time and the change of Cu in matte was less than 2 wt pct from the predicted Cu in matte.

Figure 3 provides the experimental results from different equilibration times of 0.5, 3, 24, and 48 hours.

The matte and slag compositions from the 0.5-hour experiment were taken as the “new” initial starting point. FactSage predictions using the public database^[26–30] and equilibrium trend lines obtained from present experiments with equilibration times longer than 24 hours are also plotted in Figure 3.

The compositional variation after a 0.5-hour equilibration is consistent with the expected trend in matte compositional movement from low to high Cu, as discussed in a previous publication.^[20] Figure 3 shows that the closer the matte particle is located to the

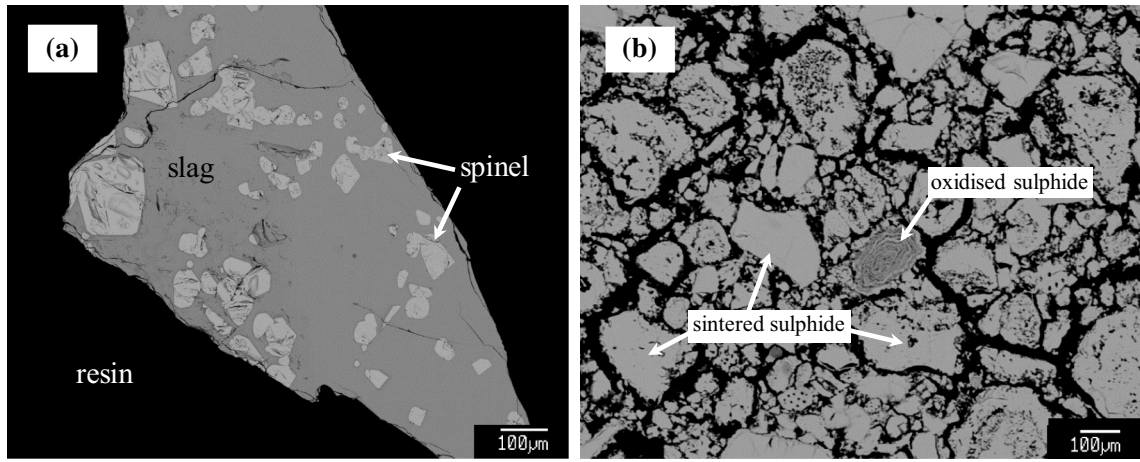


Fig. 4—SEM backscattered images showing the microstructure of the (a) master slag and (b) sintered sulfide (Table IV provides phase compositions).

gas-slag-matte interface, the greater the Cu concentration in matte; *i.e.*,

$$\begin{aligned}
 (\text{Cu in matte})_{b'-\text{matte}} &\approx (\text{Cu in matte})_{b-\text{matte}} \\
 &> (\text{Cu in matte})_{f-\text{matte}} \\
 &> (\text{Cu in matte})_{d-\text{matte}} \\
 &> (\text{Cu in matte})_{c-\text{matte}} \\
 &> (\text{Cu in matte})_{a-\text{matte}} \\
 &> (\text{Cu in matte})_{g-\text{matte}}.
 \end{aligned}$$

Figure 3 also shows that the slag composition followed the spinel liquidus composition corresponding to the composition of the nearest matte. The closer the slag is located to the gas-slag-matte interface, the lower its FeO and S concentrations; *i.e.*,

$$(\text{FeO})_{B-\text{slag}} < (\text{FeO})_{A-\text{slag}} \text{ and } (\text{S})_{B-\text{slag}} < (\text{S})_{A-\text{slag}}.$$

The matte and slag compositions at different locations from 24- and 48-hours experiments were the same within the experimental uncertainty, *i.e.*, less than ± 1.1 wt pct at 1473 K (1200 °C), $P(\text{SO}_2) = 0.25$ atm, and $P(\text{O}_2) = 10^{-8.5}$ atm (Figures 3(a) through (d)). This indicates that the reactions between the gas, slag, and matte phases were completed after 24 hours.

Several important points are shown by these initial experiments. (1) The assumption that the reaction between slag and matte phases is more rapid than the reaction between gas-condensed phases is valid. Slag and matte compositions in close physical proximity always follow the experimental equilibrium trend lines (Figures 3(b) through (d)), while gas and matte phases require significant time to attain equilibrium (Figure 3(a)). (2) The *b'*- and *b*-matte and *B*-slag locations represent phases that already achieved the equilibrium condition or phases with the closest compositions to the phases at the equilibrium condition. (3) When the initial Cu in matte is ± 20 wt pct lower than the equilibrium value, 24-hour equilibration time is sufficient for the gas/slag/matte/spinel phases to reach

the equilibrium point. When the initial Cu in matte is closer to the equilibrium point, shorter equilibration time is needed.

D. Equilibration Experiment with Master Slag and Sintered Sulfide

An experiment with master slag and sintered Cu-Fe sulfide was also performed to confirm the equilibrium slag and matte compositions. The master slag was prepared by equilibrating an oxide mixture at 1473 K (1200 °C) and $P(\text{O}_2) = 10^{-8.5}$ atm for 24 hours. The sintered sulfide was prepared by annealing a sulfide mixture at 530 °C in argon atmosphere containing 10 ppm H_2 for 24 hours. The micrographs and compositions of the master slag and sintered sulfide are provided in Figure 4 and Table IV, respectively. The results given in Table V show no significant difference in matte and slag compositions between the experiment using master slag and sintered sulfide and the experiments using sulfide powders and oxide powders as starting materials.

E. Solutes in Spinel Solid Solution

The concentrations of solutes in spinel were analyzed using EPMA. The “ Cu_2O ”, S, and SiO_2 concentrations in the spinel were measured as a function of type of spinel and distance from the matte/spinel or slag/spinel interface. Figure 5 shows three different types of spinel in the sample obtained from the experiment at 1473 K (1200 °C), $P(\text{SO}_2) = 0.25$ atm, $P(\text{O}_2) = 10^{-8.0}$ atm, and equilibration time = 18 h: (1) spinel next to the matte phase (Figure 5(a)), (2) spinel within the matte phase (Figure 5(b)), and (3) spinel far from large matte particles inside the slag (Figure 5(c)). The compositional measurements on the different types of spinel were made on cross sections of the phases at 2- μm intervals.

The sulfur concentration in the spinel was below the detection limit of the present EPMA measurement, *i.e.*, 0.05 wt pct S. The SiO_2 and “ Cu_2O ” concentrations of different types of spinel as a function of distance from

Table IV. Measured Compositions of Master Slag and Sintered Sulfide

Material	Temperature (°C)	Time (h)	Condition	Normalized Oxide Composition (Wt Pct)				Old Total [†]
				“Cu ₂ O”	“FeO”	SiO ₂	S	
Master slag	1200	24	$P(O_2) = 10^{-8.5}$ atm	0.29	70.1	29.3	0.01	96.8

Material	Temperature (°C)	Time (h)	Condition	Normalized Sulfide Composition (Wt Pct)				Old Total [†]
				Cu	Fe	Si	S	
Sintered sulfide	530	24	Ar with 10 ppm H ₂	60.6	14.0	0.00	25.4	99.4

[†]“Old total” is the original sum of elements or oxides given by EPMA before it is normalized.

the spinel/matte or spinel/slag interface from the present and previous study on the Cu-Fe-O-S system^[22] are plotted in Figure 6. Figure 6(a) shows uniform SiO₂ concentrations in different types of spinel with average composition of approximately 0.75 wt pct.

Figure 6(b) shows that the “Cu₂O” concentration in spinel varies with the distance from the matte/slag interface, with the highest “Cu₂O” concentration approximately 0.85 wt pct at a 5- μ m distance from the interface. The “Cu₂O” concentrations in spinel near the matte-spinel interface from the Cu-Fe-O-S-Si and Cu-Fe-O-S systems were identical, indicating that the SiO₂ solubility in spinel does not have an effect on the Cu solubility in spinel. The spinel located in the slag phase far from the matte phase (Figure 5(c)) had the lowest “Cu₂O” concentration, *i.e.*, less than 0.1 wt pct.

It was not possible to accurately measure the copper concentrations in spinel at the spinel/slag interface. Further, the spinel in contact with the matte phase was rarely observed in the present study, unlike in the previous study of the gas/matte/spinel equilibria in the Cu-Fe-O-S system,^[22] where spinel solid was always in contact with the matte phase. The measurement results show that the representative “Cu₂O” concentration in the spinel should only be taken from the measurements of spinels in the vicinity of the matte phase, such as those shown by Figures 5(a) and (b) from the present study in the Cu-Fe-O-S-Si system or from the previous study of the gas/matte/spinel equilibria in the Cu-Fe-O-S system.^[22]

F. Independent Experimental Confirmation

Independent experiments were carried out by the co-author (A. Fallah-Mehrjardi) to confirm the present experimental result. Spinel substrate with spiral shape^[23] was employed to improve equilibration process and enhance the quenching result. The experimental results for equilibrations at 1200 °C, $P(SO_2) = 0.25$ atm, and $P(O_2) = 10^{-8.5}$ atm using two different substrate types are provided in Table V. There was no significant difference in matte and slag compositions between the trials using the two different substrate types.

G. Conditions for Equilibrium

A detailed analysis of the potential pathways for the attainment of chemical equilibrium between gas/slag/matte/spinel phases in the Cu-Fe-O-S-Si system was undertaken. The criterion of the equilibrium is the fulfillment of all conditions of the four-point test: (1) no effect of longer equilibration time, (2) homogeneity of the slag and matte phases, (3) equilibrium point confirmed by approaching from different directions, and (4) reactions identified in the samples completed. The phase equilibria data reported in the present study meet this criterion.

IV. RESULTS AND DISCUSSION

A. Complete Description of the Multicomponent, Multiphase Cu-Fe-O-S-Si System

Complete representation and analysis of the compositions of all phases in this multicomponent, multiphase system is essential to ensure high precision of the results. A similar set of graphs to those presented in the previous study for the gas/slag/matte/tridymite equilibria in the Cu-Fe-O-S-Si system^[21] was selected, which is minimum in number but sufficiently and completely describes the equilibrium between the gas and condensed phases. The set of graphs adopted in the present study describes the gas, matte, and slag in the system, all expressed as a function of Cu in matte (= $100 \cdot Cu / [Cu + Fe + S]$):

1. For the matte phase:
 - (a) $\log_{10}[P(O_2), \text{atm}]$;
 - (b) sulfur in matte (= $100 \cdot S / [Cu + Fe + S]$ (wt pct)); and
 - (c) oxygen in matte (= $100 \cdot \text{sum of Cu, Fe, and S in matte measured by EPMA (wt pct)}$).
2. For the slag phase:
 - (a) FeO in slag (= $100 \cdot FeO / [FeO + SiO_2 + Cu_2O + S]$ (wt pct));
 - (b) sulfur in slag (= $100 \cdot S / [FeO + SiO_2 + Cu_2O + S]$ (wt pct));

Table V. Measured Compositions of Phases from Slag/Matte/Tridymite Equilibria in the Cu-Fe-O-S-Si System at 1200 °C, $P(\text{SO}_2) = 0.25$ atm, Equilibration Time = 24 hours, and a Range of $P(\text{O}_2)$

No.	$\log_{10}(P(\text{O}_2, \text{Atm}))$	Equilib. Time (h)	Phase	Normalized Matte Composition (Wt Pct)			Old Total [‡]
				Cu	Fe	S	
1	- 8.60	24	matte	47.3	26.5	26.1	97.9
2	- 8.60	24	matte	42.7	31.3	25.9	95.0
3	- 8.60	24	matte	43.7	30.5	25.7	95.4
4	- 8.60	24	matte	48.1	25.8	25.7	97.4
5	- 8.60	18	matte	47.1	26.3	25.8	95.6
6	- 8.55	24	matte	53.4	21.1	25.5	97.1
7	- 8.55	24	matte	52.5	22.0	25.4	99.2
8	- 8.55	18	matte	51.1	23.9	25.0	99.7
9	- 8.55	18	matte	54.8	19.8	25.3	98.7
10	- 8.55	18	matte	50.7	24.2	25.1	97.3
11**	- 8.50	24	matte	64.5	11.9	23.6	99.0
12	- 8.50	48	matte	63.1	13.0	23.9	98.2
13	- 8.50	24	matte	63.9	12.3	23.8	100.6
14	- 8.50	24	matte	64.3	12.0	23.7	99.7
15 [†]	- 8.50	24	matte	63.7	12.5	23.7	99.6
16 [†]	- 8.50	24	matte	64.6	11.7	23.7	99.4
17	- 8.40	24	matte	69.2	8.2	22.5	100.2
18	- 8.40	24	matte	69.7	7.9	22.3	101.6
19	- 8.40	24	matte	68.3	8.9	22.8	99.1
20	- 8.30	24	matte	71.4	6.7	21.9	101.7
21	- 8.30	24	matte	72.3	6.1	21.6	102.4
22	- 8.30	24	matte	73.1	5.2	21.7	101.5
23	- 8.20	24	matte	73.5	4.9	21.6	100.9
24	- 8.20	24	matte	75.0	3.8	21.2	101.5
25	- 8.20	48	matte	75.1	3.8	21.1	102.8
26 [†]	- 8.20	24	matte	75.2	3.4	21.3	99.6
27	- 8.10	24	matte	75.9	3.2	20.9	101.4
28	- 8.00	24	matte	77.2	2.3	20.4	102.5
29	- 7.90	24	matte	78.3	1.5	20.2	103.0

No.	Phase	Normalized Oxide Composition (Wt Pct)				Old Total [‡]	Cu in Slag*	Fe/SiO ₂ in Slag
		“Cu ₂ O”	“FeO”	SiO ₂	S			
1	slag	1.82	74.4	19.6	4.1	101.9	1.61	2.95
	spinel	N/A	99.2	0.70	0.03	92.3		
2	slag	2.2	75.2	17.5	5.1	100.9	1.97	3.35
	spinel	N/A	99.2	0.68	0.01	93.2		
3	slag	2.2	74.7	18.2	4.9	101.4	1.96	3.20
	spinel	N/A	99.3	0.64	0.01	93.5		
4	slag	1.79	74.2	19.3	4.5	101.8	1.59	2.98
	spinel	N/A	99.3	0.65	0.01	93.4		
5	slag	1.82	74.5	19.2	4.4	101.3	1.62	3.02
	spinel	N/A	99.2	0.67	0.00	92.8		
6	slag	1.29	72.9	22.8	3.0	100.7	1.14	2.48
	spinel	N/A	99.2	0.73	0.00	93.2		
7	slag	1.55	74.0	20.9	3.4	101.2	1.38	2.75
	spinel	N/A	99.2	0.66	0.02	92.6		
8	slag	1.48	73.9	20.9	3.8	101.2	1.31	2.75
	spinel	N/A	99.2	0.73	0.01	94.0		
9	slag	1.33	72.3	23.5	2.9	100.7	1.18	2.39
	spinel	N/A	99.3	0.67	0.00	93.3		
10	slag	1.70	73.9	20.3	3.8	100.8	1.51	2.84
	spinel	N/A	98.9	0.69	0.01	93.5		
11**	slag	0.96	71.4	25.4	1.66	99.2	0.85	2.18
	spinel	N/A	98.4	0.70	0.01	93.7		

Table V. continued

No.	Phase	Normalized Oxide Composition (Wt Pct)				Old Total [‡]	Cu in Slag*	Fe/SiO ₂ in Slag
		“Cu ₂ O”	“FeO”	SiO ₂	S			
12	slag	1.14	71.7	25.2	1.92	100.7	1.01	2.21
	spinel	N/A	99.2	0.76	0.01	93.4		
13	slag	1.00	70.2	27.2	1.58	99.8	0.89	2.01
	spinel	N/A	99.3	0.61	0.00	93.5		
14	slag	0.99	70.5	26.9	1.56	99.8	0.88	2.03
	spinel	N/A	99.1	0.75	0.01	93.7		
15 [†]	slag	1.16	72.0	24.8	1.99	100.4	1.03	2.26
	spinel	N/A	99.3	0.66	0.00	93.2		
16 [†]	slag	1.07	70.7	26.5	1.72	99.1	0.95	2.07
	spinel	N/A	99.2	0.75	0.00	92.4		
17	slag	0.92	69.0	29.0	1.06	99.2	0.82	1.85
	spinel	N/A	99.1	0.82	0.00	92.3		
18	slag	0.88	69.0	29.1	0.98	100.4	0.79	1.84
	spinel	N/A	99.2	0.73	0.00	93.8		
19	slag	0.95	69.7	28.0	1.25	100.0	0.84	1.93
	spinel	N/A	99.2	0.81	0.00	92.0		
20	slag	0.95	67.8	30.3	0.82	100.2	0.84	1.74
	spinel	N/A	99.2	0.57	0.01	93.2		
21	slag	0.97	68.5	29.8	0.73	100.4	0.86	1.79
	spinel	N/A	99.2	0.83	0.00	93.5		
22	slag	0.93	67.8	30.5	0.70	99.8	0.82	1.72
	spinel	N/A	99.3	0.57	0.01	93.0		
23	slag	1.03	67.0	31.4	0.57	100.5	0.91	1.66
	spinel	N/A	99.1	0.75	0.02	93.6		
24	slag	0.94	66.7	31.8	0.48	99.8	0.84	1.63
	spinel	N/A	99.2	0.74	0.01	93.0		
25	slag	0.91	66.9	31.5	0.51	100.7	0.81	1.65
	spinel	N/A	99.2	0.67	0.01	94.3		
26 [†]	slag	0.91	65.6	33.0	0.46	97.9	0.81	1.55
	spinel	N/A	99.6	0.31	0.03	90.2		
27	slag	1.05	66.6	31.7	0.39	99.8	0.93	1.63
	spinel	N/A	99.2	0.68	0.01	94.0		
28	slag	1.14	65.7	32.9	0.27	99.7	1.01	1.55
	spinel	N/A	99.2	0.76	0.00	92.1		
29	slag	no liquid slag						
	spinel	N/A	99.2	0.69	0.02	93.4		
	tridymite	0.13	0.67	99.2	0.00	101.6		

Concentrations of elements less than 0.1 wt pct are below the detection limit of the present EPMA measurement.

*Cu (copper loss in slag) is recalculated from concentration of Cu₂O in the slag phase ($Cu = [2M_{Cu}/M_{Cu2O}] \cdot Cu_2O / [Cu_2O + FeO + SiO_2 + S]$).

**Experiment using master slag and sintered sulfide as starting materials.

[†]Independent confirmation experiments by co-author.

[‡]“Old total” is the original sum of elements or oxides given by EPMA before it is normalized.

(c) Cu in slag (= $100 \cdot Cu / [FeO + SiO_2 + Cu_2O + S]$ (wt pct)); and

(d) Fe^{3+} / Fe_{Total} in slag.

Each of the graphs contains experimentally measured values, previously reported results for the gas/slag/matte/tridymite equilibria in the Cu-Fe-O-S-Si system by Fallah et al.,^[21] previous results for the gas/matte/spinel equilibria in the Cu-Fe-O-S system,^[22] and predicted values using FactSage software with the public database.^[26–30] Weight rather than mole percent was selected for ease of practical application of the experimental results.

B. Experimental Results of the Gas/slag/matte/spinel Equilibria in the Cu-Fe-O-S-Si System at 1473 K (1200 °C), at $P(SO_2) = 0.25$ atm, and in a Range of $P(O_2)$

Experiments were performed at 1473 K (1200 °C) and $P(SO_2) = 0.25$ atm for a range of oxygen partial pressures and equilibration time of 24 hours, or shorter times in the case of samples with initial Cu concentrations in matte close to the equilibrium point. All of the measured phase compositions are summarized in Table V and plotted in Figure 7. The matte and slag compositions were obtained from EPMA measurements at the gas/slag/matte interface (*b'*- and *b*-matte and

B-slag). The spinel compositions were obtained, where possible, from the EPMA measurements of spinels in the vicinity of the matte phase.

1. $P(O_2)$ vs Cu in matte

Figure 7(a) shows that the Cu in matte increases with increasing oxygen partial pressure. The Cu in matte changes from approximately 45 wt pct (at $P(O_2) = 10^{-8.6}$ atm) to approximately 78 wt pct (at $P(O_2) = 10^{-7.9}$ atm) in less than 1 unit $\log_{10}[P(O_2), \text{atm}]$ scale. The Cu in matte becomes very sensitive to $P(O_2)$ at conditions below $10^{-8.5}$ atm. As a result, the precision of the measurement of the Cu in matte decreases with decreasing Cu in matte. For example, the variations of Cu in matte at $P(O_2) = 10^{-8.5}$, $10^{-8.55}$, and $10^{-8.6}$ atm are ± 1.1 , ± 2.0 , and ± 3.5 wt pct,

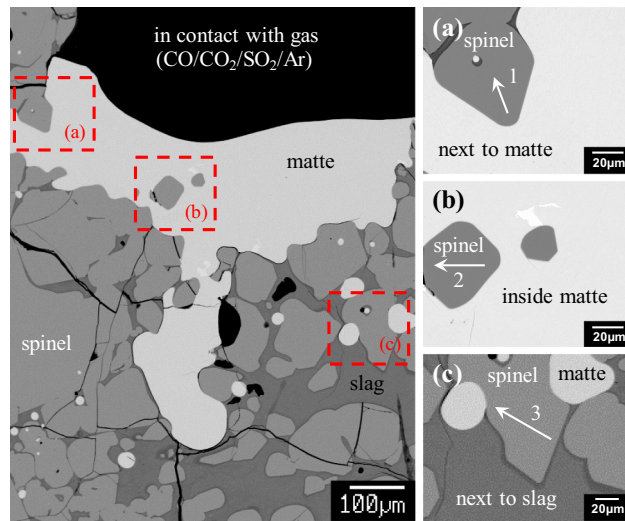


Fig. 5—SEM backscattered image showing spinel at different locations in the sample from gas/matte/spinel equilibria in the Cu-Fe-O-S-Si system at 1473 K (1200 °C), $P(SO_2) = 0.25$ atm, $P(O_2) = 10^{-8.0}$ atm, and equilibration time = 18 h: (a) spinel next to matte, (b) spinel inside matte, and (c) spinel next to slag.

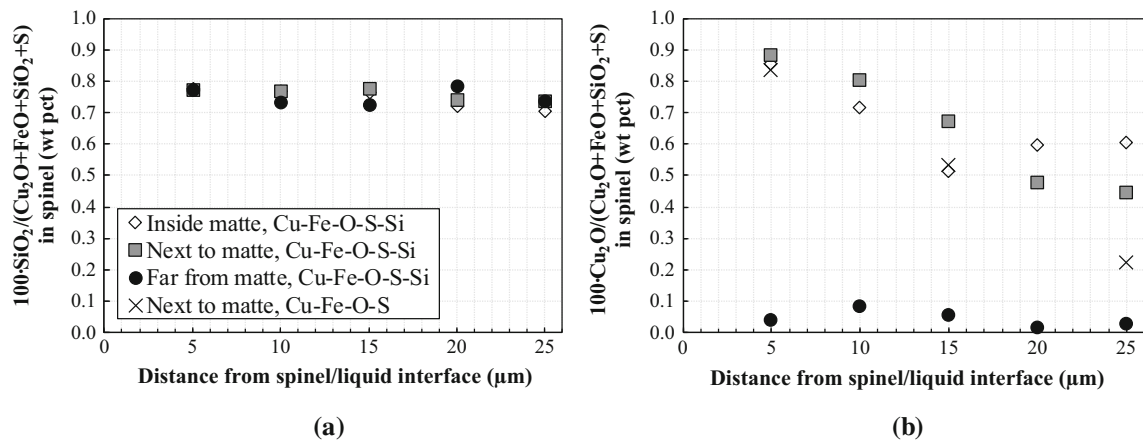


Fig. 6—Concentrations of solutes in spinel as a function of distance from the spinel/matte or spinel/slag interface in the sample prepared for gas/matte/spinel equilibria in the Cu-Fe-O-S-Si system at 1473 K (1200 °C), $P(SO_2) = 0.25$ atm, $P(O_2) = 10^{-8.0}$ atm, and equilibration time = 18 h. Experimental data for Cu-Fe-O-S are from Ref. [22]: (a) SiO_2 concentration in spinel and (b) “ Cu_2O ” concentration in spinel.

respectively (Figure 7(a')). This is in agreement with the previous findings in the gas/matte/spinel equilibria by the authors.^[22] Compared to that from the gas/slag/matte/tridymite equilibria,^[21] the gas/matte/spinel equilibria correspond to higher $P(O_2)$ for a given Cu in matte. The FactSage predicted lines with the public database^[26–30] give a similar trend but overestimate the absolute $P(O_2)$ values in both equilibria.

2. S in matte vs Cu in matte

Figure 7(b) shows that the sulfur in matte increases, following the Cu_2S-FeS stoichiometric line, with decreasing Cu in matte from 77 to 55 wt pct. At Cu in matte below 55 wt pct, the sulfur in matte vs Cu in matte relationship departs from the Cu_2S-FeS stoichiometric line (hypothetical line of S in matte vs Cu in matte established from mixing stoichiometric Cu_2S and FeS); i.e., the matte becomes increasingly sulfur deficient. The relationship of sulfur in matte and Cu in matte obtained in the present study is identical to those reported in previous studies for the gas/matte/spinel equilibria^[22] and in the gas/slag/matte/tridymite equilibria.^[21] The departure from stoichiometric compositions is not described by the FactSage public database.^[26–30]

3. Dissolved oxygen in matte vs Cu in matte

The oxygen concentrations in the matte were estimated by taking the difference between 100 and the sum of Cu, Fe, and S in matte measured by EPMA. The sums of measured elements at high Cu in matte were more than 100, resulting in negative values for the oxygen concentrations; this appears to be related to the EPMA measurement uncertainties.

Figure 7(c) shows a qualitative relationship between oxygen dissolved in the matte and Cu in the matte. In general, the present and previous results^[21,22] show an increase in the oxygen dissolved in the matte with increasing iron in matte. The oxygen concentrations in the matte for a given Cu in matte at the gas/slag/matte/spinel and gas/matte/spinel^[22] equilibria are higher than those for the gas/slag/matte/tridymite equilibria.^[21]

The increase in the oxygen concentration in matte with decreasing oxygen partial pressure appears to be counterintuitive. The ability of iron to form an oxy-sulfide liquid is related to the high O solubility in the matte phase at lower Cu in matte. The increase of O in matte leads to the departure of sulfur in matte from the stoichiometric line, as shown in Figure 7(b). The observed difference in the trend of sulfur in matte as a function of Cu in matte between the present results and the FactSage prediction is related to the absence of oxygen in the matte solution of the public database.^[26–30]

4. FeO in slag vs Cu in matte

Figure 7(d) shows the “FeO” concentration in the slag in equilibrium with spinel. The “FeO” in slag decreases significantly with increasing Cu in matte. This indicates a significant increase of spinel stability with increasing $P(\text{O}_2)$. It can be observed that the FactSage prediction^[26–30] consistently overestimates the “FeO” in liquid slag by 2 wt pct. The “FeO” in the spinel-saturated slag converges to the “FeO” in the tridymite-saturated slag^[21] at the slag solidus point at this temperature, at which gas/matte/spinel/tridymite phase assemblage is present.

5. Dissolved sulfur in slag vs Cu in matte

The concentration of sulfur dissolved in slag at spinel saturation is inversely related to the Cu in matte, as shown in Figure 7(e). The sulfur in slag changes from approximately 5 to 0.3 wt pct when Cu in matte increases from approximately 43 to 77 wt pct. The sulfur solubility in the spinel-saturated slag at fixed Cu in matte is always higher than the sulfur solubility in the tridymite-saturated slag.^[21] FactSage with public database^[26–30] reproduces the trends; however, it underestimates the absolute values up to 2 wt pct.

6. Chemically dissolved copper in slag vs Cu in matte

The chemically dissolved copper in the slag as a function of Cu in matte is given in Figure 7(f). The lowest copper solubility in slag is observed at Cu in matte of approximately 70 wt pct. At Cu in matte higher than 70 wt pct, the copper in slag increases, which appears to be due to an increase in the “oxidic” dissolution of copper in the slag. At Cu in matte lower than 70 wt pct, the copper in slag significantly increases, which may be related to the increase in the so-called “sulfidic” dissolution of copper in the slag.^[31] At a given Cu in matte, the copper solubility in the spinel-saturated slag is higher than that in the tridymite-saturated slag. Further investigation is needed to confirm the trend of chemically dissolved copper in the slag at Cu in matte lower than 40 wt pct. FactSage with public database^[26–30] does not reproduce the trends and underestimates the absolute values of copper in slag over the entire range of Cu in matte.

7. Fe^{+3}/Fe ratio in slag vs Cu in matte

Figure 7(g) shows the ratio of Fe^{+3} to the total iron predicted using FactSage with the public database.^[26–30] The predictions show that the proportion of Fe^{3+} in

slag increases with increasing Cu in matte. The Fe^{3+} in the slag in equilibrium with spinel is consistently higher than that in the slag in equilibrium with tridymite. The Fe^{3+} concentration is an important parameter in that it represents the capacity of the slag to absorb oxygen beyond the anticipated for stoichiometric FeO. Currently, there is no accurate data of Fe^{3+} in slag at the gas/slag/matte/spinel equilibria in the Cu-Fe-O-S-Si system.

8. Composition of spinel

The sulfur concentration in the spinel is below the detection limit of the present EPMA measurement. The average SiO_2 concentration in spinel is approximately 0.75 wt pct and appears not to be sensitive to change in Cu in matte (Table V). Representative “ Cu_2O ” concentrations in the spinel were not obtained in the present study. The “ Cu_2O ” concentration in the spinel as a function of Cu in matte should be taken from the previous study of the gas/matte/spinel equilibria in the Cu-Fe-O-S system.^[22] The total composition of the spinel is less than 100 wt pct (between 90.2 and 94.3 wt pct). This is because of the recalculation of all iron in the oxide phases to FeO, selected for the representation of the experimental results, since neither oxygen nor iron oxidation states were measured with EPMA in the present study.

9. Fe/SiO₂ ratio and sulfur capacity in slag

The Fe/SiO₂ ratios and sulfur capacities of the slags are given in Figures 8(a) and (b), respectively. Figure 8(a) shows the Fe/SiO₂ ratios in the slag at the liquidus of the spinel and tridymite^[21] primary phase fields decrease with increasing Cu in matte. In between the two liquidus lines, the matte is in equilibrium with fully liquid slag (no solid oxide is formed).

The sulfur capacity in the slag, C_s , is defined as^[32]

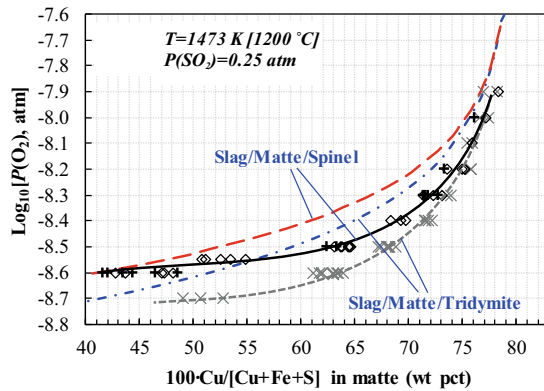
$$C_s = [\text{S}] (P(\text{O}_2)/P(\text{S}_2))^{0.5}, \quad [7]$$

where [S] is the weight percent of dissolved sulfur in the slag phase measured by EPMA (Table V) and $P(\text{O}_2)$ and $P(\text{S}_2)$ are the respective oxygen and sulfur partial pressures of the gas phase in equilibrium with the slag phase (in atmosphere). The $P(\text{S}_2)$ is calculated based on the $\text{O}_{2(\text{gas})} + 0.5\text{S}_{2(\text{gas})} = \text{SO}_{2(\text{gas})}$ equilibrium, where

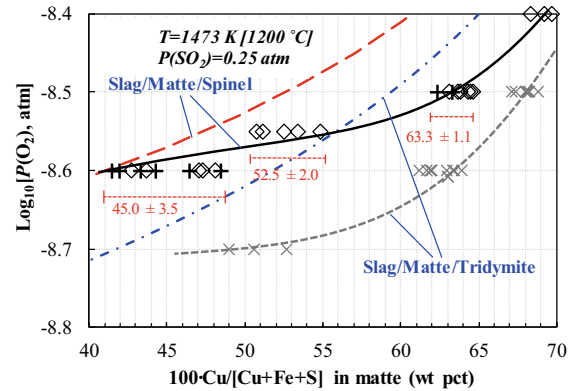
$$K_{1473\text{ K}} = \frac{P(\text{SO}_2)}{P(\text{O}_2) \times (P(\text{S}_2))^{0.5}} = 1.04 \times 10^9, \quad [8]$$

where K is the equilibrium constant calculated using FactSage.^[26–30] $P(\text{SO}_2)$ is the sulfur dioxide partial pressure in the gas phase (in atmosphere).

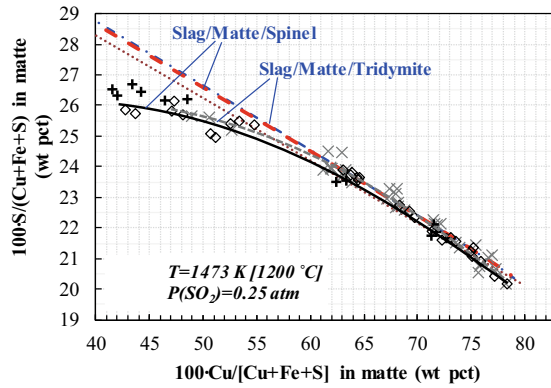
The calculated sulfur capacity is inversely proportional to the Cu in matte, as shown in Figure 8(b). For the given Cu in matte, the calculated value of sulfur capacity in the present study is higher than that in the gas/slag/matte/tridymite equilibria.^[21] Revision of the public database^[26–30] of FactSage is required to improve the description of the gas/slag/matte/solid equilibria in the Cu-Fe-S-O-Si system.



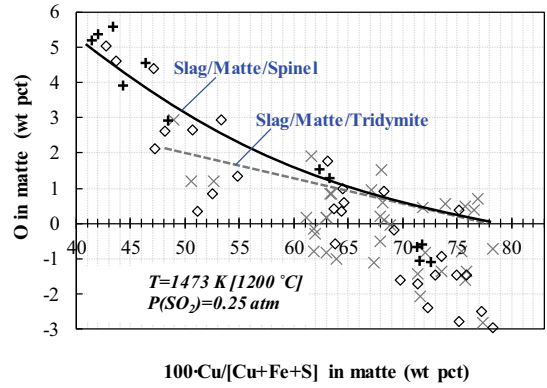
(a)



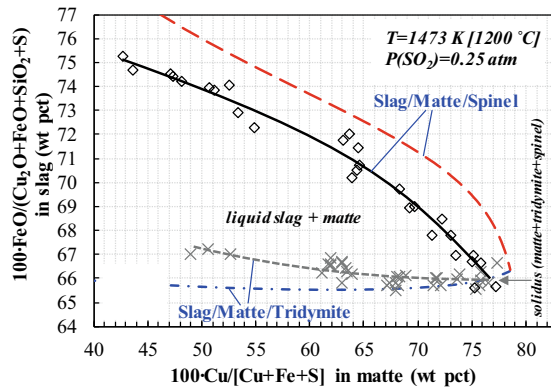
(a')



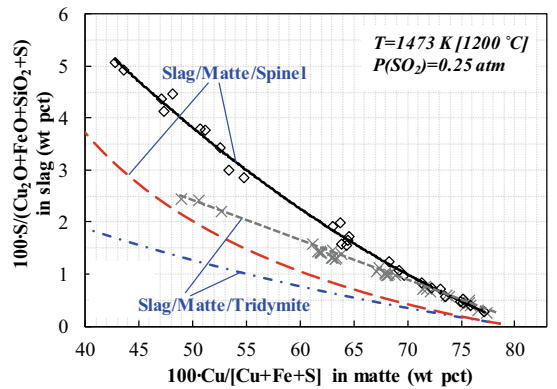
(b)



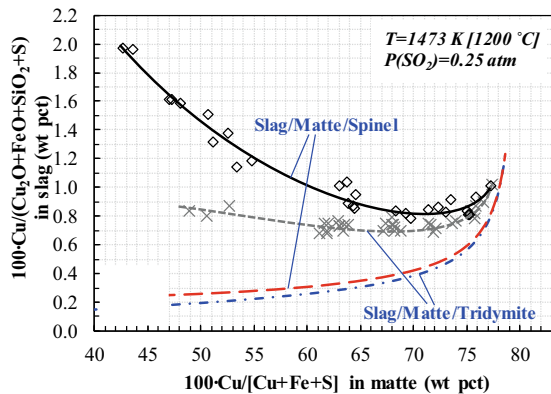
(c)



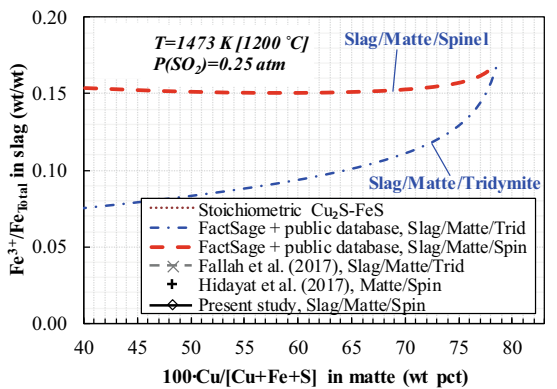
(d)



(e)



(f)



(g)

◀ Fig. 7—Set of graphs describing the gas/slag/matte/spinel equilibria in the Cu-Fe-O-S-Si system at 1473 K (1200 °C), $P(\text{SO}_2) = 0.25$ atm, and a range of $P(\text{O}_2)$: (a) oxygen partial pressure ($P(\text{O}_2)$, atm) vs Cu in matte; (a') detail of oxygen partial pressure ($P(\text{O}_2)$, atm) vs Cu in matte; (b) concentration of sulfur in matte vs Cu in matte; (c) concentration of oxygen in matte vs Cu in matte; (d) FeO in slag vs Cu in matte; (e) concentration of sulfur in slag vs Cu in matte; (f) concentration of copper in slag vs Cu in matte; and (g) ferric iron to total iron ratio in slag vs Cu in matte. Previous data are from Refs. [21] and [22]. Dashed lines are FactSage predictions using the public database.^[26–30]

10. Comparison with previous studies

Several studies were carried out previously to investigate the gas/slag/matte/spinel equilibria in the Cu-Fe-O-S-Si system at 1473 K (1200 °C) and $P(\text{SO}_2) = 0.25$ atm. Henao *et al.*,^[16] and Sun and Jak^[17] employed a similar experimental technique to that used in the present study. There are several differences in the details of the approaches used in the previous studies,^[16,17] such as the following.

- (1) The starting chemicals used in these previous studies were metals and oxide powders. Sulfur was introduced into the condensed phases by reaction with the gas phase.
- (2) The equilibration experiments in the previous studies were performed in less than 6 hours equilibration time.
- (3) Molybdenum wire was used to hold samples in the furnace, causing some contamination.
- (4) A fully focused or zero-diameter beam was used for the EPMA compositional measurement of all phases, including for the matte and slag phases.

These differences create potential uncertainties in the experimental results. The use of metal powder and the introduction of sulfur from the gas phase to create matte phase may require an equilibration time longer than 6 hours. The use of a zero-diameter beam can give nonrepresentative composition of nonfully homogeneous phase, such as matte phase or slag phase.

Comparison between the present and the previous results^[16,17] is provided in Figure 9. Figure 9(a) shows that the reported Cu amounts in matte by Henao *et al.*,^[16] at $P(\text{O}_2) = 10^{-8.0}$ atm and Sun and Jak^[17] at $P(\text{O}_2) = 10^{-8.6}$ atm are consistent with the Cu in matte from the present study at the corresponding $P(\text{O}_2)$. A difference in the Cu in matte can be observed between Sun and Jak's data and the present result at $P(\text{O}_2) = 10^{-8.3}$ atm.

Figure 9(b) shows that the sulfur in matte reported by Henao *et al.*,^[16] is significantly lower than the sulfur in matte from the present study. Sun and Jak^[17] did not provide measurements of the sulfur concentration in the matte phase.

Figure 9(c) shows that the Fe/SiO₂ ratios in slag from Henao *et al.*,^[16] and Sun and Jak^[17] at high Cu in matte are consistent with those from the present study. Significant differences in the Fe/SiO₂ ratio in slag can be observed between Sun and Jak's data and the present result at low Cu in matte.

Figure 9(d) compares the concentrations of dissolved copper in the slag reported in the previous^[16,17] and current studies. The figure demonstrates the improved precision and accuracy of the measurements obtained with the methodology used in the present study.

V. IMPLICATIONS

The system investigated in the present study is directly relevant to the industrial copper making practice, where silica is used as a flux material and slag is free of Al₂O₃, CaO, and MgO. The conditions correspond closely to those experienced during the slag-blow process in the Peirce–Smith converter.

During the slag-blow, matte and Cu-bearing materials are oxidized with air until there is approximately 1 wt pct Fe left in the molten matte.^[33] Iron is oxidized and fluxed with silica, forming iron-silicate slag. The process temperature fluctuates around 1473 K (1200 °C).^[34] If there

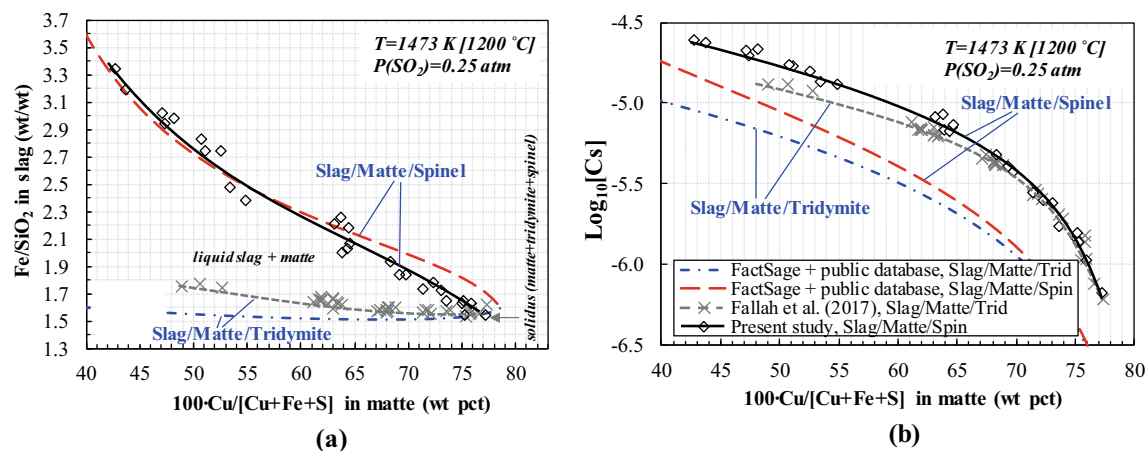


Fig. 8—Gas/slag/matte/solid equilibria in the Cu-Fe-O-S-Si system at 1473 K (1200 °C) and $P(\text{SO}_2) = 0.25$ atm: (a) Fe/SiO₂ ratios vs Cu in matte and (b) sulfur capacities of the slags vs Cu in matte. Previous data are from Refs. [21] and [22]. Dashed lines are FactSage predictions using the public database.^[26–30]

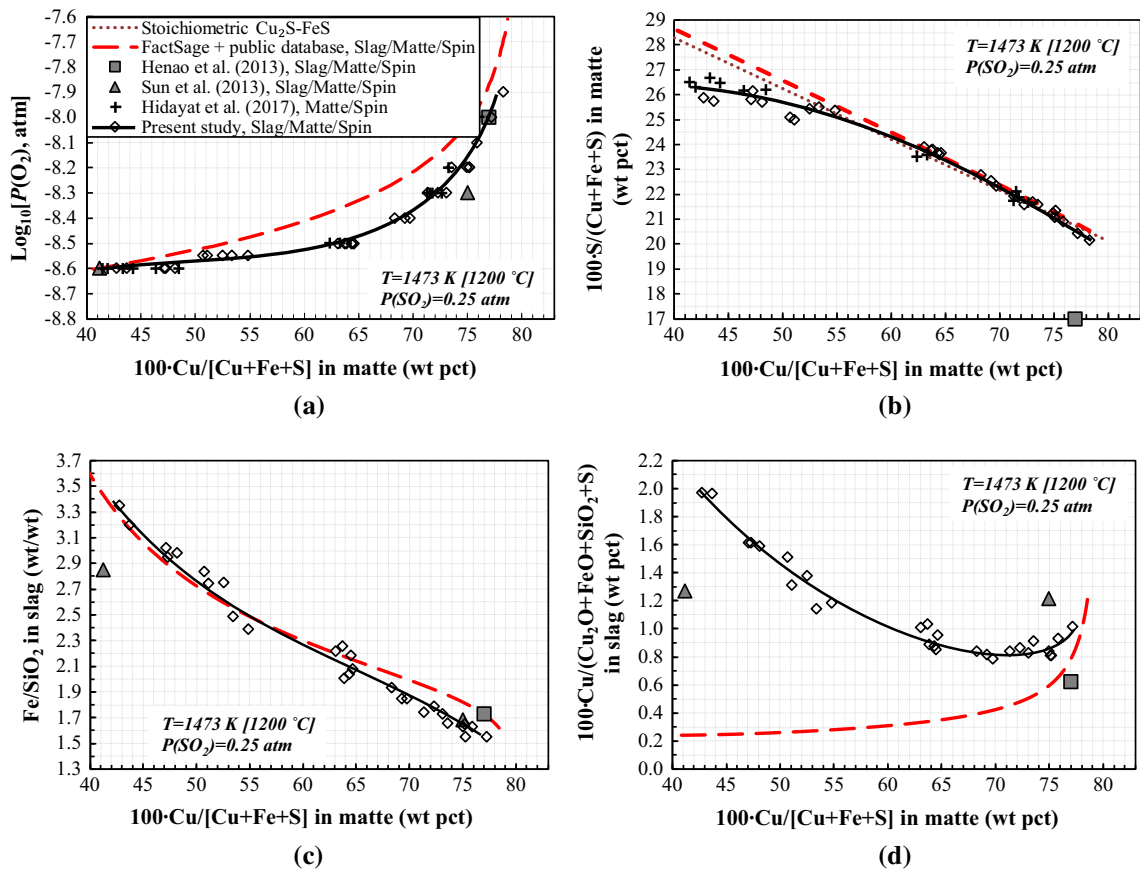


Fig. 9—Set of graphs describing the gas/slag/matte/spinel equilibria in the Cu-Fe-O-S-Si system at 1473 K (1200 °C), $P(\text{SO}_2) = 0.25 \text{ atm}$, and a range of $P(\text{O}_2)$: (a) oxygen partial pressure ($P(\text{O}_2)$, atm) vs Cu in matte; (b) concentration of sulfur in matte vs Cu in matte; (c) Fe/SiO₂ ratio in slag vs Cu in matte; and (d) concentration of copper in slag vs Cu in matte. Previous data are from Henao *et al.*,^[16] and Sun and Jak^[17] Dashed lines are FactSage predictions using the public database.^[26–30]

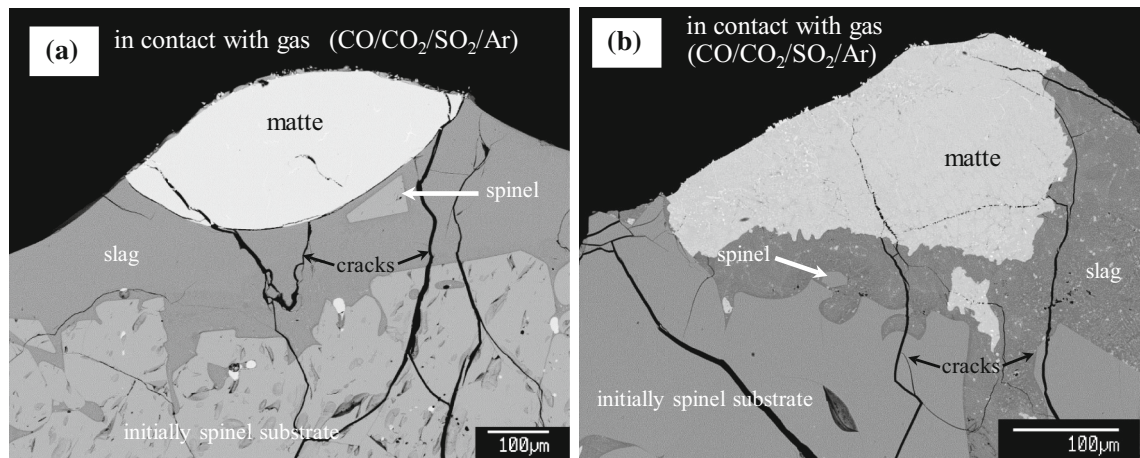


Fig. 10—SEM backscattered electron images of samples from gas/slag/matte/spinel equilibria in the Cu-Fe-O-S-Si system at 1473 K (1200 °C), $P(\text{SO}_2) = 0.25 \text{ atm}$, and Cu in matte: (a) above 60 wt pct and (b) below 60 wt pct.

is little or no slag retained and recycled in the converter, the concentrations of Al₂O₃, CaO, and MgO in slag will be low,^[11,34] and Figure 8(a) can be used as a guide to fluxing practice. The figure shows that the operating window for a fully liquid slag is inversely proportional to the Cu in matte. The operating window area decreases as the

converting process progresses. Fe/SiO₂ ratio in slag needs to be adjusted by the addition of SiO₂ to ensure slag is fully liquid or has a low proportion of solid. Control of the SiO₂ addition is required to avoid overfluxing, at which point slag reaches SiO₂ saturation, slag viscosity is high, and more smelting heat is required.^[11,34,35] For example, at

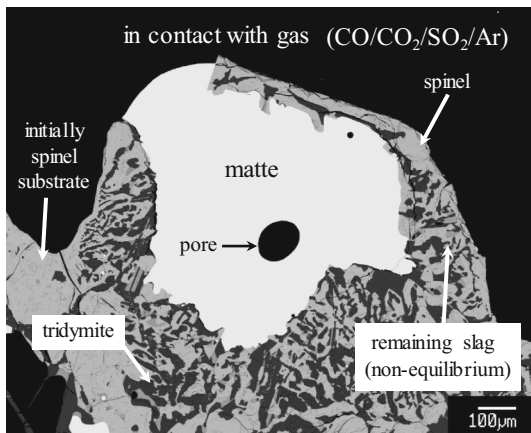


Fig. 11—SEM backscattered electron image of sample from gas/slag/matte/spinel equilibria in the Cu-Fe-O-S-Si system at 1473 K (1200 °C), $P(\text{SO}_2) = 0.25$ atm, and $P(\text{O}_2) = 10^{-7.9}$ atm (Cu in matte above 78 wt pct).

1473 K (1200 °C), $P(\text{SO}_2) = 0.25$ atm, and 70 wt pct Cu in matte, the Fe/SiO₂ ratio in slag must be maintained between 1.55 and 1.85 wt/wt in order to obtain a fully liquid slag or slag with low proportion of solid.

Figure 10(a) shows a microstructure of the sample with Cu in matte above 60 wt pct, and Figure 10(b) shows a microstructure of the sample with Cu in matte below 60 wt pct. It can be observed that the slag/matte interface for the low Cu in matte is more irregular compared to that for the high Cu in matte. The irregularity of the slag/matte interface at low Cu in matte indicates a decrease in interfacial tension between matte and slag with decreasing Cu in matte; this was quantitatively measured in a previous study.^[36] The decrease in the interfacial tension between the matte and slag can lead to poor separation between these phases.^[37] This indicates that smelting with low target Cu in matte should be avoided to reduce the physical matte entrainment in the slag. The low Cu in matte also contributes to the high chemical copper loss in the slag, as can be seen in Figure 7(f).

Figure 11 shows a microstructure of the sample from the equilibration experiment at 1473 K (1200 °C), $P(\text{SO}_2) = 0.25$ atm, and $P(\text{O}_2) = 10^{-7.9}$ atm. It can be observed that the liquid slag was completely solidified, resulting in the matte/spinel/tridymite phase assemblage. This finding reflects an overblowing condition in the converter furnace. The situation can be avoided by increasing the furnace temperature or by avoiding the overblowing through monitoring of the composition final matte product.

The present study provides information on the Cu-Fe-O-S-Si system. The presence of additional components in the form of Al₂O₃, CaO, and MgO, which in practice are introduced in raw materials, fluxes, and refractory materials, influences the elemental distributions between slag, matte, and spinel phases. Further information on the effect of these components will be provided in future publications by the authors.

VI. CONCLUSIONS

The improved experimental methodology based on equilibration, rapid quenching of equilibrium phases, and EPMA analysis of the phases was used to investigate the gas/slag/matte/spinel equilibria in the Cu-Fe-O-S-Si system at 1473 K (1200 °C), $P(\text{SO}_2) = 0.25$ atm, and a range of $P(\text{O}_2)$. The four-point-test approach was employed to confirm the equilibrium achievement in the present study. The approach involved the evaluation of the (1) effect of equilibration time, (2) homogeneity of equilibrated phases, (3) effect of direction of achievement of equilibrium, and (4) analysis of reactions specific to the system. Confirmation by independent experiments and analysis of solid-state diffusion of solutes in spinel solid were also undertaken in this study.

A set of key graphs was introduced to describe the equilibrium in the multicomponent, multiphase system Cu-Fe-O-S-Si. The graphs provide information on $P(\text{O}_2)$ in gas, S in matte, O in matte, Fe/SiO₂ in slag, S in slag, Cu in slag, and $\text{Fe}^{3+}/\text{Fe}_{\text{Total}}$ in slag, all presented as functions of Cu in matte. Comparisons between the present results, previous results in the gas/slag/matte/tridymite,^[21] previous results in the gas/matte/spinel^[22] equilibria, and FactSage prediction are provided. The experimental data in the present study can be used for the evaluation of effects of oxidation condition and fluxing on the slag liquidus, percent solid, and chemical copper loss in the slag. The new data can also be used as input for the revision of the thermodynamic database for the copper-containing systems.

ACKNOWLEDGMENTS

The authors thank the Australian Research Council Linkage program LP140100480, Altonorte Glencore, Atlantic Copper, Aurubis, BHP Billiton Olympic Dam Operation, Kazzinc Glencore, PASAR Glencore, Outotec Oy (Espoo), Anglo American Platinum, Umicore, and Rio Tinto Kennecott for the financial and technical support for this research. They also acknowledge the support of the AMMRF at the Centre for Microscopy and Microanalysis, University of Queensland.

REFERENCES

1. N. Korakas: Ph.D. Thesis, Université de Liège, Liège, 1964.
2. U. Kuxmann and F.Y. Bor: *Erzmetallurgie*, 1965, vol. 18, pp. 441–50.
3. F.J. Tavera and W.G. Davenport: *Metall. Trans. B*, 1979, vol. 10B, pp. 237–41.
4. H. Li and W.J. Rankin: *Metall. Mater. Trans. B*, 1994, vol. 25B, pp. 79–89.
5. Y. Takeda: *Proc. 5th Int. Conf. Molten Slags, Fluxes and Salts*, Iron and Steel Society, Warrendale, PA, 1997.
6. G. Roghani, M. Hino, and K. Itagaki: *Mater. Trans. JIM*, 1997, vol. 38, pp. 707–13.
7. J.M. Font, G. Roghani, M. Hino, and K. Itagaki: *Metall. Rev. MMIJ*, 1998, vol. 15, pp. 75–86.
8. G. Roghani, Y. Takeda, and K. Itagaki: *Metall. Mater. Trans. B*, 2000, vol. 31B, pp. 705–12.

9. H.M. Henaio, L.A. Ushkov, and E. Jak: *Proc. 9th Int. Conf. Molten Slags, Fluxes and Salts*, The Chinese Society for Metals, Beijing, 2012.
10. Z. Sun, T. Hidayat, P. Hayes, and E. Jak: *Proc. 8th Int. Copper Conf.*, Chilean Institute of Mining Engineers, Santiago, 2013.
11. N. Cardona, P.J. Mackey, P. Coursol, R. Parada, and R. Parra: *JOM*, 2012, vol. 64, pp. 546–50.
12. H.N. Lander: Ph.D. Thesis, Massachusetts Institute of Technology, Cambridge, MA, 1954.
13. T. Rosenqvist and T. Hartvig: *Norges Tek.-Naturvitenskapelige Forskiningsrud Met. Kom. Meddel.*, 1958, pp. 21–52.
14. F. Johannsen and H. Knahl: *Z. Erzbergbau Metallhuettenwes.*, 1963, vol. 16, pp. 611–21.
15. D.L. Kaiser and J.F. Elliott: *Metall. Trans. B*, 1988, vol. 19B, pp. 935–41.
16. H.M. Henaio, P.C. Hayes, and E. Jak: Pyrosearch, The University of Queensland, Private Communication, 2013.
17. Z. Sun and E. Jak: Pyrosearch, The University of Queensland, 2013.
18. E. Jak, P.C. Hayes, and H.-G. Lee: *Met. Mater. (Seoul)*, 1995, vol. 1, pp. 1–8.
19. E. Jak: *Proc. 9th Int. Conf. Molten Slags, Fluxes and Salts*, The Chinese Society for Metals, Beijing, 2012.
20. A. Fallah-Mehrjardi, T. Hidayat, P.C. Hayes, and E. Jak: *Metall. Mater. Trans. B*, 2017, vol. 48B, pp. 3002–16.
21. A. Fallah-Mehrjardi, T. Hidayat, P.C. Hayes, and E. Jak: *Metall. Mater. Trans. B*, 2017, vol. 48B, pp. 3017–26.
22. T. Hidayat, P. Hayes, and E. Jak: *J. Phase Equilib. Diff.*, 2017, <https://doi.org/10.1007/s11669-018-0616-5>.
23. T. Hidayat, A. Fallah Mehrjardi, P. Hayes, and E. Jak: *10th Int. Conf. Molten Slags, Fluxes and Salts*, TMS, Seattle, WA, 2016.
24. T. Hidayat, A. Fallah Mehrjardi, P.C. Hayes, and E. Jak: *9th Int. Copper Conf.*, The Mining and Materials Processing Institute of Japan & Japan Mining Industry Association, Kobe, 2016.
25. T. Hidayat, D. Shishin, E. Jak, and S. Decterov: *CALPHAD*, 2015, vol. 48, pp. 131–44.
26. E. Jak, S.A. Decterov, P.C. Hayes, and A.D. Pelton: *Proc. 5th Int. Conf. Molten Slags, Fluxes and Salts*, Iron and Steel Society, Sydney, 1997.
27. S.A. Decterov and A.D. Pelton: *Metall. Mater. Trans. B*, 1999, vol. 30B, pp. 661–69.
28. E. Jak, S.A. Decterov, B. Zhao, A.D. Pelton, and P.C. Hayes: *Metall. Mater. Trans. B*, 2000, vol. 31B, pp. 621–30.
29. S.A. Decterov, I.-H. Jung, E. Jak, Y.-B. Kang, P.C. Hayes, and A.D. Pelton: *7th Int. Conf. Molten Slags, Fluxes & Salts*, The South African Institute of Mining and Metallurgy, Cape Town, 2004.
30. FactSage 7.0: *FToxid and FTmisc databases*, <http://www.factsage.com/>, 2015.
31. F. Sehnalek and I. Imris: *Proc. Advances in Extractive Metallurgy and Refining*, Institution of Mining and Metallurgy, London, 1972.
32. M. Allibert, H. Gaye, J. Geiseler, D. Janke, B.J. Keene, D. Kirner, M. Kowalski, J. Lehmann, K.C. Mills, D. Neuschütz, R. Parra, C. Saint-Jours, P.J. Spencer, M. Susa, M. Tmar, and E. Woermann: *Slag Atlas*, Verlag Stahleisen GmbH, Dusseldorf, 1995.
33. W.G.I. Davenport, M. King, M. Schlesinger, and A.K. Biswas: *Extractive Metallurgy of Copper*, 4th ed., Pergamon Press, Oxford, 2002.
34. P. Tan: *Int. J. Mater. Res.*, 2007, vol. 98, pp. 995–1003.
35. D. Shishin, T. Hidayat, S. Decterov, and E. Jak: *Proc. 10th Int. Conf. Molten Slags, Fluxes and Salts*, TMS, Seattle, WA, 2016.
36. J.F. Elliot and M. Mounier: *Can. Metall. Q.*, 1982, vol. 21, pp. 415–28.
37. A.I. Belyaev: *Surface Phenomena in Metallurgical Processes*, Consultants Bureau, New York, NY, 1965.